Evaluation of Electrical Impedance Tomography for the Localization of Lung Nodules

A THESIS
SUBMITTED TO THE FACULTY OF THE GRADUATE SCHOOL
OF THE UNIVERSITY OF MINNESOTA
BY

GOLAM RAKIB MAZUMDER

IN PARTIAL FULFILLMENT OF THE REQUIREMENTS
FOR THE DEGREE OF
Master Of Science

ADVISOR: Dr. MICHAEL GREMINGER

August, 2020

Acknowledgements

There are many people that I have to thank in my graduate school. I am highly thankful to my advisor Dr. Michael Greminger for taking me in his group and giving me an opportunity to work with him. When I started the journey of my master's thesis, I was not confident enough whether I can complete the thesis. My very first thanks for the completion of this thesis goes to Dr. Greminger for his organized and focused guidance from learning the basic to advanced knowledge needed for the thesis. He always steered me in the right direction. He greatly helped me with his perceptive thoughts about the progress I was making to finish my research. I am also grateful for his super guidance and support in my PhD application which helped me a great deal to earn a PhD fellowship. My appreciation also extends to my research colleagues Gills Fai and Kinyee Sin.

I can't thank enough my parents who have gone through much struggles from my early childhood for my education and for inspiring me to go for higher education. I thank them for supporting me even at this stage of my life being 8000 miles away. I am also thankful to my sister and my nephews for their love and support when I was struggling with my problems. Truth to be told, the completion of this thesis would not have been possible without the immense love and support I received from my family members.

It is my pleasure to show my sincere gratitude to Dr. Brian Hinderliter and Dr. Desineni Naidu for being kind enough to be in my thesis committee. I want to thank them for giving me constructive reviews and right direction to complete the thesis. I would also like to thank Dr. Robert Palumbo and Dr. Alison Hoxie for their support and guidance with completing my MS program at Duluth.

I would like to thank my colleague and friend Labiba Imtiaz, now pursuing MS at

the University of Minnesota Duluth, who has helped me to improve my writing. She always helped me in many aspects that I cannot list them all. Thank you. I also like to thank Shougat, Sudipta, Maqsood, and Touhid for their unconditional support.

I want to thank Kim and Tracy for their administrative help and I would also like to thank the Swenson College of Science and Engineering for the funding and support.

It is my great pleasure to show my sincere gratitude to my all time favorite teacher and personality - Professor Md. Ashiqur Rahman, my undergrad supervisor, who has an immense contribution to the journey of my life both academically and philosophically.

Finally, I am highly thankful to the Almighty for blessing me with the strength of passing through this path, facing all the obstacles with confidence and courage.

Dedication

To my nephews Anan & Ayan.

Abstract

The objective of this study was to investigate whether tomography can be used to localize lung cancer modules to guide biopsies conducted through a bronchoscope. The dielectric properties of cancerous lung tissue are different from normal lung tissue. Hence, impedance across the electrodes in lung cancer biopsy tools will vary. Simulation in Ansys Q3D of a 3D structure of a lung biopsy tool containing array of electrodes was performed and it was found that the impedance for the normal lung case was higher than the cancer lung case at both 1 KHz and 1 MHz frequencies and at different electrode positions. To support the simulation results, the use of gelatin phantoms for simulating dielectric properties of lung tissues were experimentally investigated. Gelatin phantoms were composed of pure gelatin, sodium chloride and water. Among all the compositions, sample numbers 5 and 8 closely matched the dielectric properties of normal and cancer lung tissue. A prototype probe containing four pairs of electrodes was used in these samples to calculate the total impedance. Consistently, variations of electrical impedance at different electrode positions and frequencies were observed.

Contents

List of Tables

List of Figures

Chapter 1

Introduction

1.1 Background

1.1.1 Lung Cancer Statistics

According to the American Cancer Society, cancer cases have the second highest death rate compared to other death cases in the United States. According to Siegel et al., (2017)[5], the total cancer incidence from 2004-2013, was stable in women but decreased by 2% for men. Also, the overall death rate dropped by 25% due to early detection methods and treatments. Despite the advances in surgical treatment, lung cancer is still one of the leading causes of death from malignant diseases worldwide. According to the American Cancer Society, from 2009 to 2015, the 5 year relative survival rate for the lung and bronchus cases was 19%, a very low survival rate. The American Cancer Society estimates there will be 228,820 new lung and bronchus cancer cases and 135,720 deaths in 2020, ranking first and second among all cancer cases [6].

1.1.2 Lung Biopsy Tools

Early detection of cancer often allows for better treatment and higher survival rate. A CT scan of the chest can reveal small abnormal areas of the lungs called pulmonary nodules. Not all of the lung nodules in those CT scans are cancerous [7]. To determine if lung nodules are cancerous, a biopsy needs to be done. If these nodules are located in the center of the lungs, this can be done easily using a standard bronchoscope. But

it's difficult when nodules are located at the periphery of the lung [3]. To overcome this problem, electromagnetic navigation bronchoscopy (ENB) and endobronchial ultrasound (EBUS) systems can be used. The ENB system was introduced to overcome the shortcomings of conventional lung biopsy tools. ENB helps the physician navigate the biopsy tool to the periphery of the lung. It creates an electromagnetic field to identify the exact location of a probe inside the patient's chest [8]. However, this procedure is costly and time consuming compared to traditional bronchoscopy and leads to additional radiation exposure to the patient. EBUS is a new addition to the diagnosis method of the bronchoscopist and a highly effective method to determine if the biopsy tool is adjacent to a long nodule using ultrasound [9].

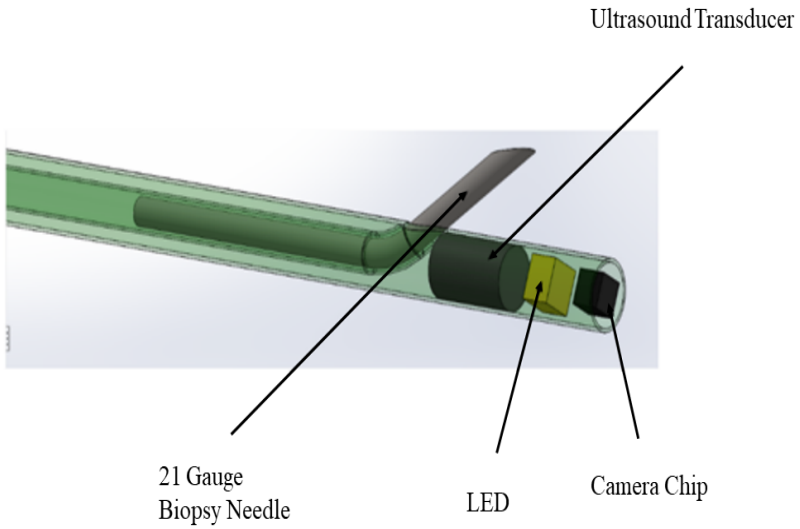

Figure 1.1: Lung Biopsy Tool device [3]

Transbronchial Biopsies of Peripheral Lung Nodules

Fai et al., 2019 [3] proposed a concept to work with the existing version of endobronchial ultrasound transducers (EBUS) probes (Fig 1.1). This proposed lung biopsy tool device is combined with an ultrasound transducer, camera and flexible 21 gauge biopsy needle making it economically feasible and disposable. But the EBUS transducer is too expensive to be included in a disposable device.

One solution to this problem is to make two channels in the proposed biopsy tool as shown in the fig. 1.2. One channel is for the biopsy needle and second channel is for the reusable EBUS probe. The biopsy needle is composed of high strength polymer and its end is designed in such a way that it can be deployed near the EBUS probe. This proposed design allows the EBUS probe and biopsy needle to be deployed simultaneously. Also, the LED and the camera are positioned co-axially to make the tool smaller. The tool can be made even smaller if the camera module and EBUS probe are designed to be interchangeable. This design allows the EBUS probe and the camera to be swapped, as the camera can be used to identify the correct lung portion and then removed to insert the EBUS module.

One of the disadvantages of this design was sizing. When the EBUS channel was adjacent to the needle channel, the design was forced to have a larger diameter. This idea was one of the motivations for using electrical impedance to make the overall diameter of the tool smaller like in fig. 1.3.

1.1.3 Dielectric Properties of Lung Tissue

The human body is a complex biological structure of living tissue. Biological cells contain intracellular fluids, cell membranes and tissues, and that exhibit frequency dependent behavior on electrical signals. Hence, biological cells and tissues produce an electrical bio-impedance. Bioimpedance measurements are widely accepted as a low cost, non-invasive, safe, no radiation and quantitative analytical method to identify the status of benign and malignant biological tissues [10]. Due to the dielectric properties of thin cells and tissue membranes, they have a high resistivity and behave as small capacitors electrically. Wang et al., 2014[2] investigates dielectric properties difference of normal and cancerous human lung tissues from 100 Hz to 100 MHz. For air filling

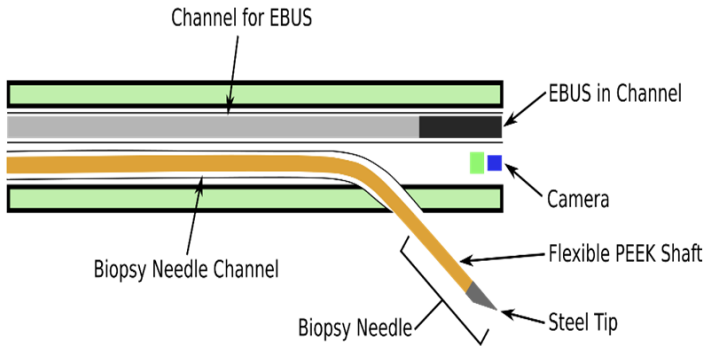

Figure 1.2: Biopsy tool with separate channel for biopsy needle and EBUS module. The flexible needle design is also shown. Biopsy tool with interchangeable EBUS model and camera module [3].

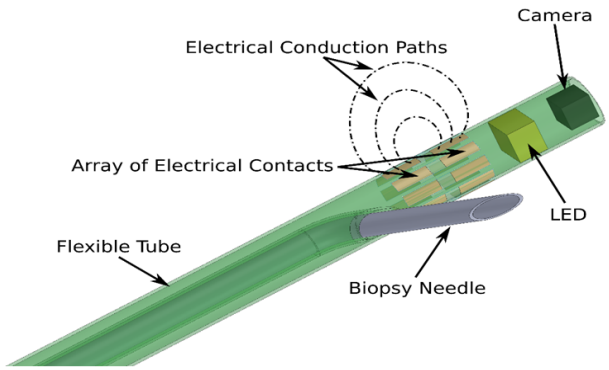

Figure 1.3: Electrical impedance probes added to biopsy tool to detect the location of lung nodules

factor, F=0.1781, he found that relative permittivity of cancerous tissue is 1.2-3 times larger than normal tissue. Also, electric conductivity of cancerous tissue is 1.6-2 times larger than that of normal tissue. Hence, the electrical impedance of tissues can be used as a sensing modality for normal and cancer tissues.

1.1.4 Gelatin Phantom Model

A tissue-mimicking phantom that accurately represents tissue properties, is important for safety testing, quality assurance and as well as verification for any treatment techniques. Marchal et al., 1989[11] suggested the use of gelatin phantoms for simulating the dielectric properties of human tissues. They are easy to make, low cost and have properties in the same order of magnitude of soft tissues. These phantoms are made of gelatin, water and different amount of sodium chloride (NaCl). For example, at 37°C and 27 MHz, it was found that the electrical conductivity of gelatin at concentrations of 10% to 40% was 0.27 to 0.45 S/m. At the same concentration, the relative permittivity was 87 to 100 [11]. So, for easy and low cost simulation of most human tissues for different frequencies, gelatin made of water and NaCl is used for experiments.

1.2 Thesis Objectives and Outline

The purpose of this thesis is to determine if the impedance tomography can be used to locate lung cancer modules to guide tumor lung biopsies, conducted through a bronchoscope. It's an alternative sensing modality to locate malignant lung tissues, which rectifies the existing EBUS transducer (fig. 1.3). Since the electrical properties of lung nodules are different from normal lung tissue, this technique can be used to determine whether the biopsy tool is adjacent to the lung nodules. To test this idea, a gelatin model was implemented to mimic the dielectric properties of normal and cancerous lung tissues.

The structure of the thesis goes as follows:

- Chapter 1 discusses different lung biopsy tools, dielectric properties of lung tissue, gelatin phantom model and introduces the objectives of the thesis.
- Chapter 2 briefly discusses the related literature and motivation of the thesis.

- Chapter 3 describes the simulation process used in the analysis.
- Chapter 4, the gelatin phantom experiment is outlined.
- Chapter 5 presents final results from simulation and experimental works.
- Chapter 6 is about conclusion of the analyses presented in the thesis.

Chapter 2

Literature Review

The dielectric properties are most often found on healthy lung tissue at different frequencies. Durney et al., (1986)[12] as well as Foster and Schwan (1996)[13] experimented on human ex vivo lung tissues and got data for relative permittivity and conductivity at room temperature. Gabriel (1996)[14] made a database of dielectric properties of human skin, bone and cartilage, liver and kidney tissue at low to high frequency. Later, this comprehensive database based on large number of tissue helped to shed new light on bioimpedance. Also, Joines et al., (1994)[15] experimented on normal and malignant human body tissues to calculate electrical conductivity and relative permittivity from 50 to 900 MHz. Kimura et al., (1994)[16] experimented on pulmonary mass of 53 patients to measure electrical impedance. From those data, needle biopsy technique was used to determine the location of the biopsy needle within the pulmonary mass. Wang et al., (2014)[2] studied the dielectric properties of human lung tissue at the frequencies of 100 Hz to 100 MHz in normal and cancer cases. The relative permittivity of cancer tissue is 1.2-3 times higher than normal tissue and for conductivity it's 1.6-2 times higher. Significant differences in the dielectric properties, provide data for the impedance measurement for human lung tissue. Cao et al., (2014)[17] measured the average of real and imaginary parts of electrical impedance from 91 patients with lung cancer. Using two characteristic equations (Cole-Cole circle radius and complex modulus), most normal and cancerous tissues were correctly classified and identified. Borsic et al., (2010)[18] introduced the Transrectal Electrical Impedance Tomography (TREIT) for prostate imaging. The TREIT probe used the array of electrodes on the

surface of ultrasound probe inside the imaging volume.

A brief overview of the historical progress of impedance based on cell measurement is given as follows:

Table 2.1: Historical overview in impedance-based cell measurement

Early 1930s	Computed impedance of several single marine eggs and frog eggs over the frequency range from 1 to 2500 KHz[19, 20].
1956	Wallace Coulter invented impedance measurement at zero frequency (DC current) for blood analysis and cell volume measurement[21].
1979	Cell impedance properties measurement using AC signal at high frequency[22].
1984	Measured electrical impedance properties of fibroblast, cultured on gold electrodes that was subjected to alternating electric field[23].
1993-2000	Fabrication of micro-scale electrodes and fluid channels[24, 25, 26].
2006	Use of an imaging tool, Electrical Impedance Tomography (EIT) in clinical diagnosis and it's future developments [27]
2013	Use of dielectric spectroscopy for cell and tissue characterization and analysis [28].

In the field of lung biopsy tool design, many studies have been conducted on the usability and reliability of ENB and EBUS procedures. Lamprecht et al., (2012)[29] conducted observational study of 112 patients to evaluate the diagnostic yield of ENB combined with CT and determined the factors associated with diagnostic yield. ENB increased the diagnostic rate of traditional standard bronchoscopy to 70%, while the diagnostic rate is 53%. Seijo (2016)[8] also studied different aspects of ENB as a clinical utility tool for lung cancer diagnosis. Eberhardt et al.,(2007)[9] introduced multimodal

bronchoscopy diagnosis, combination of EBUS and ENB. The goal was to overcome the limitations of each individual and increase the diagnostic yield. The combination of EBUS and ENB improved the diagnostic yield of flexible bronchoscopy in peripheral lung nodules without compromising safety. Hsia et al., (2012)[30] also proved that the radial EBUS navigation improved the diagnostic yield of bronchoscopy. Adler and Boyle (2017)[31] used EIT to image the electrical properties through electrical simulations applied to electrodes. The goal was to find the correlation between EIT images and electrical properties of tissue. Fai et al., (2019)[3] proposed the idea of using the reusable EBUS probe in existing EBUS system which was briefly explained in 1.1.2.

Gelatin phantom is used to mimic the conditions found in human tissues, using everyday and cheap materials. Marchal et al., 1989[11] suggested the use of gelatin phantoms made of gelatin, water and NaCl for simulating the dielectric properties of human tissues. Nicholson and Crofton (1997)[32] used gelatin phantom simulation to practice freehand needle guidance. Kato and Ishida (1987)[33] demonstrated the agar powder which was supplemented with polyvinyl chloride (PVC) and sodium azide (NaN_3) to increase their preservation capacity. The conductivity was varied between 0.02 to 1.23 S/m and permittivity was varied between 35 to 80 in the range of 5 to 40 MHz.

Chapter 3

Simulation Work

3.1 Definitions

3.1.1 Electrical Impedance

Since the late 1800s, electrical impedance measurements have been used to study biological tissue. Numerous studies have been done using complex impedance measurements; an overview has been described in Ross, J. (1987), Macdonald, Impedance Spectroscopy [34]. According to this, the real and reactive components of biological tissue can be measured with great accuracy as they are highly conductive over the frequency range of interest. Let us consider a simple circuit (Fig3.1,) with an AC power source, a resistor, an inductor, and capacitor. To calculate impedance, we have to find resistance of the resistor and reactance of the capacitor and inductor.

Capacitor reactance can be calculated by following equation:

$$X_c = \frac{1}{2\pi f C} \tag{3.1}$$

where X_c is the total reactance due to capacitor, which is measured in Ohms (Ω), f is the frequency of the signal through capacitor, and C is the capacitance.

To calculate inductor reactance, following equation can be used:

$$X_L = 2\pi f L \tag{3.2}$$

where X_L is the total reactance due to inductor, which is measured in ohms (Ω), f is the frequency of the signal through inductor, and L is the inductance.

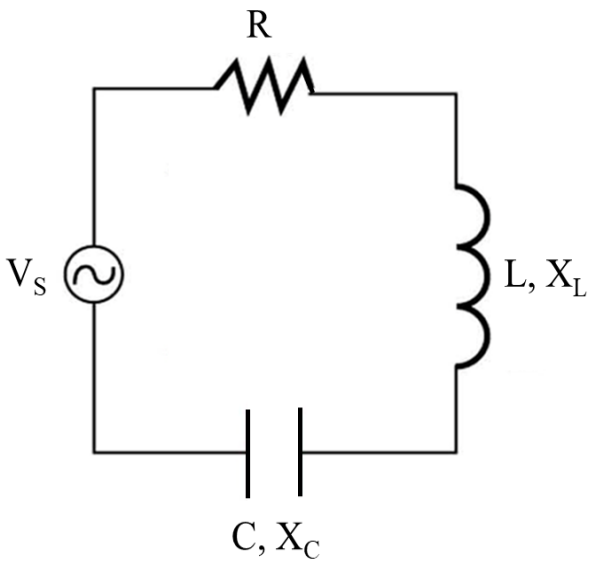

Figure 3.1: A series AC circuit with a resistor (R), inductor (L), and capacitor (C)

From impedance triangle equation, total impedance (Z) can be measured by following equation.

$$Z = \sqrt{R^2 + (X_L - X_c)^2} \tag{3.3}$$

3.1.2 Dielectric Properties

Tissue impedance consists of both electrical conductivity (σ) and dielectric terms (ϵ) due to the free and bound charges respectively [35]. Let us consider a DC power source (V), applied across parallel plate capacitor (Fig 3.2). A and t are the area of the capacitor plates and the distance between them respectively.

Capacitance without dielectric:

$$C_0 = \frac{A\epsilon_0}{t}$$

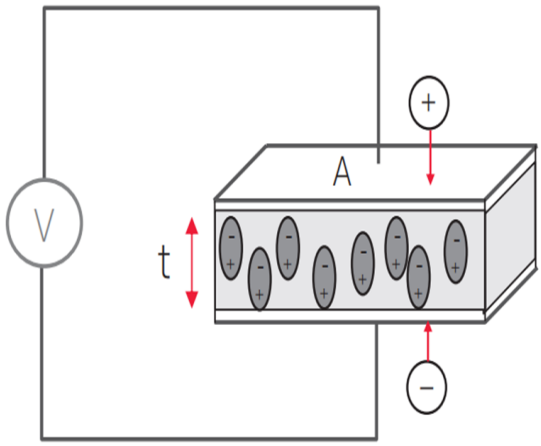

Figure 3.2: Parallel plate capacitor, DC case [4]

Capacitance with dielectric (K'):

$$C = C_0 K'$$
$$\text{where,} \quad K' = K\epsilon_0$$

Here, the constant ϵ_0 is the permittivity of free space. It's numerical value in SI units is ϵ_0 = 8.85e-12 F/m. The units of F/m are equivalent to C^2/Nm^2.

$$K' = \epsilon_r' = \frac{C}{C_o}$$

here, ϵ_r' is real dielectric constant or permittivity.

With some arrangement,

$$C = k\epsilon_0 \frac{A}{t} \tag{3.4}$$

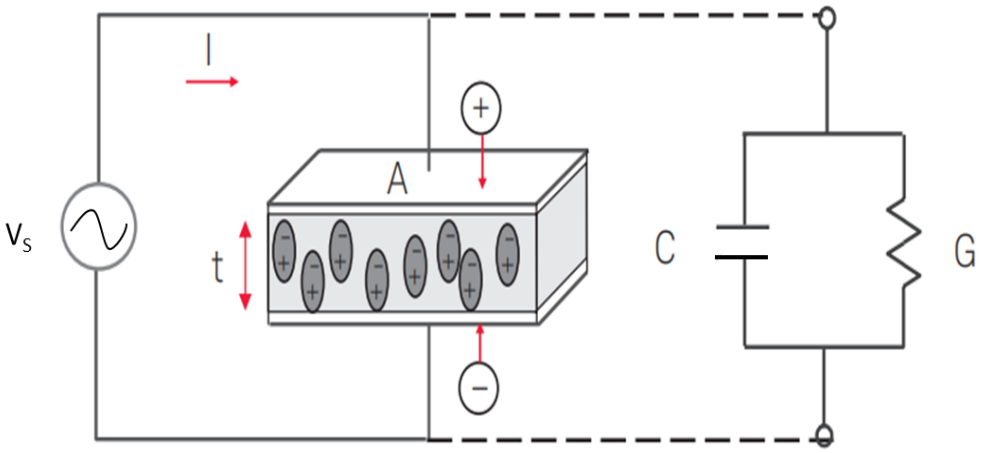

Figure 3.3: Parallel plate capacitor, AC case [4]

The dielectric material increases capacitor storage capacity. The relationship between capacitance of the dielectric material and dielectric constant is shown in equation 3.4.

If AC sinusoidal voltage (V_S) is used instead of DC voltage (V) (Fig 3.3), total current (I) will be summation of charging current (I_c) and loss current (I_L) that is related to dielectric constant [4].

$$I = I_c + I_L \tag{3.5}$$

From eq 3.1, $I_c = V_S(j\omega C)$ where angular frequency $\omega = 2\pi f$ and $C = C_0 K'$
Also according to ohm's law, $I_L = V_S G$ where Conductance $G = \omega C_o K''$

Finally equation 3.5 converts into,

$$I = V_S(j\omega \mathrm{C}_o)(K' - K'')$$

The dielectric properties of the material can be found from it's complex relative permittivity.

$$K = K' - jK'' \tag{3.6}$$

where K' is relative permittivity of the material and K'' is out of phase loss factor [14] such that,

$$K'' = \frac{\sigma}{K_o \omega} \tag{3.7}$$

Here in eq 3.7, σ is the total electric conductivity of the material and it's SI unit is Siemens per metre (S/m). K_o is the permittivity of the free space which is expressed in Farads per metre (F/m). In eqn 3.4, 3.6 and 3.7, the relationship between capacitance of the material, dielectric properties of the material and electric conductivity can be found. That's why dielectric and electric conductivity properties of biological tissues (in this thesis, lung tissue) are used as a characteristic parameters for normal and cancer tissues at different frequencies.

3.2 Description of Simulation Setup

Ansys Q3D Extractor is a 3D quasi-static solver which is used for extraction of resistance (R), partial inductance (L), capacitance (C) and conductance (G). The Q3D Extractor simulation process flow contained the following steps:

- Design of a 3D structure: Fig 3.5(1(a)) was designed in solid modeling software and different material properties were selected for all the parts in Q3D.
- Boundaries: The electrodes were designed as thin conductor. So Cu was selected as a thin conductor and it's thickness were 0.0001 inch.
- Assigned Nets: Electrodes were selected as auto nets because rest of the probe was taken as non-conductive materials.
- Solution Set Up: CG (capacitance and conductance) and AC RL (AC simulation for resistance and inductance) were selected as solution set up because the purpose was to get capacitance from CG and ac conductance from AC RL set up.

3.2.1 Verification of Q3D Simulation

Ansys Q3D was used for simulating conductance and capacitance for design simulation. Before that, a trial run was done to verify the process. Resistance of a straight copper wire (fig 3.4a) and capacitance of two parallel plates (fig 3.4b) were simulated using Ansys Q3D and comparison was done against theoretical equations. DC

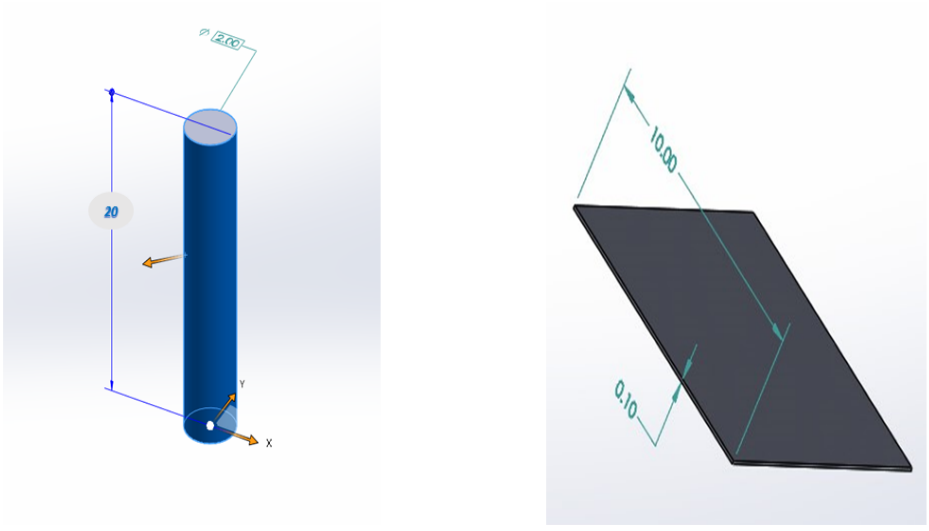

Figure 3.4: (a) A straight Cu wire (b) Two parallel plates

resistance of a copper (Cu) wire can be calculated by following equations:

$$R = \rho \frac{L}{A}$$
$$A = \frac{\pi}{4} d^2$$

where dimensions of that Cu wire (fig 3.4a): Length, L=20 mm, Diameter, d=2 mm and resistivity (ρ) of Cu wire at 25°C=1.678E-08 and frequency f= 1 MHz.

Capacitance of two parallel plates can be calculated by using equation 3.4. Dimension of parallel plate (fig 3.4b) is 10*10*0.1 (all in mm) with a thin conductor (Cu) with

dielectric constant K=10 and ϵ_0=8.85e-12 F/m.

Table 3.1: Comparison of AC and DC resistance between theoretical equation and Q3D. Calculation of theoretical AC resistance was done in online portal[1]

	Theoretical Equation	Ansys Q3D Simulation	Relative Error
DC Resistance (Ω)	0.1068	0.10903	2.09%
AC Resistance at 1 MHz(Ω)	0.00085	0.00083	2.35%
Parallel Plate Capacitance (pf)	88.54	89.56	1.15%

It is evident in table 3.1 that values of resistance and capacitance from Q3D simulation are quite accurate in comparison of standard values and relative error for all cases are around 2%. So, Ansys Q3D can be used for simulation of our system design to get the value of conductance and capacitance. In all cases, value of inductance are in nanohenry which makes X_L (eqn 3.2) quite negligible compared to X_C.

3.2.2 Probe Design

The purpose of this design was to replicate a design as if a lung biopsy tool containing electrodes was inserted into a bronchoscope. Figure 1.3 shows the concept of using electrical impedance measurements across electrodes. The phase and amplitude of the current that flows through the electrodes can be used to calculate the electrical impedance across the electrodes. The impedance depends on conductivity and permittivity of the lung and bronchiole conductivity and permittivity that surround the electrodes. Using that idea, a 3D structure (figure 3.5a) was designed using solid modeling software. Design of probe containing six electrodes and prototype of the probe that was used in experimental work were shown in figure 3.5 and figure 1.3 respectively. Specifications of the Probe and properties of the simulation 3D structure design are given below:

- Length of the 3D structure was 10 mm (figure 3.5a).
- Inner diameter of silicon probe was 2 mm and outer diameter was 2.2 mm (figure 3.5b). Relative permittivity of the silicon probe was 11.9 and electric conductivity was 0. Inside of the silicon probe was air.

- Inner diameter of the cartilage or bronchiole tube was 4 mm and outer was 4.2 mm (figure 3.5a). Relative permittivity of the tube was 32,000 and electric conductivity was 0.174 S/m [36]. Air was taken into consideration in between silicon probe and bronchiole tube.
- Diameter of lung tissue (around the bronchiole tube) for the simulation process was 8 mm. A table containing the properties of the lung tissue that were used in simulation is given in table 3.2.

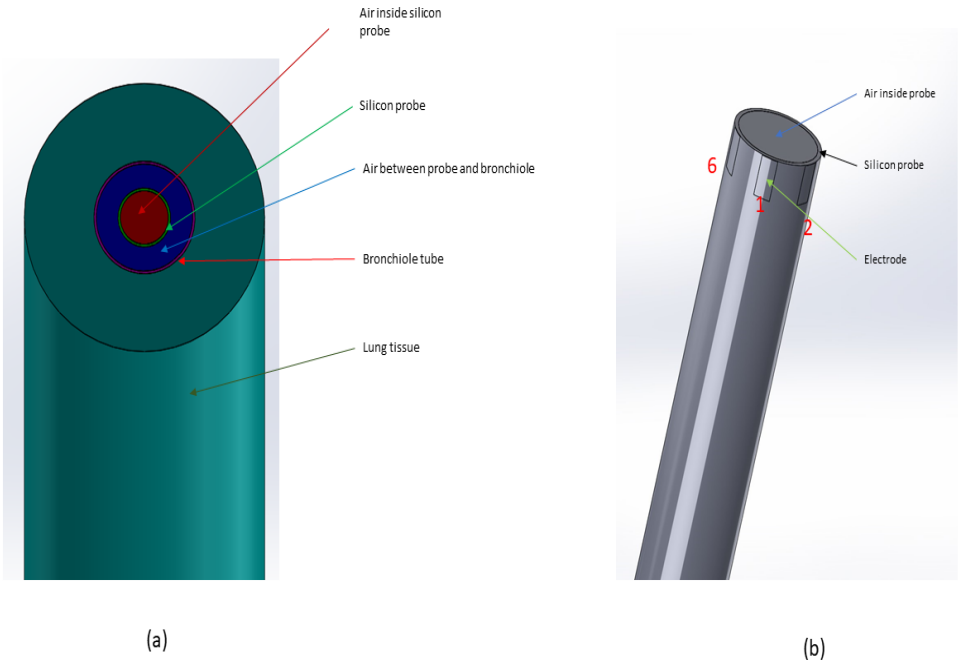

Figure 3.5: (a) Design used for simulation in ANSYS Q3D (b) Prototype of Probe showing six (1,2,3,4,5,6) electrodes

3.2.3 Results obtained from Ansys Q3D simulation

The objective of this simulation study was to investigate the electrical impedance of electrodes for normal and cancer lung tissue cases at 1 MHz and 1 KHz frequencies respectively.

Table 3.2: Dielectric properties of cancerous and lung tissues that were used in Ansys Q3D simulation and experimental comparison [2]

Frequency (Hz)	Relative Permittivity	Conductivity (S/m)	
1 KHz	200000	0.16	Normal lung tissue
	550000	0.32	Cancer lung tissue
10 KHz	30000	0.18	Normal lung tissue
	41000	0.34	Cancer lung tissue
100 KHz	4500	0.2	Normal lung tissue
	8000	0.36	Cancer lung tissue
1 MHz	1000	0.28	Normal lung tissue
	1200	0.45	Cancer lung tissue

Table 3.3 and 3.5 shows the change of capacitance and conductance of different electrodes for normal and cancerous cases at 1 MHz and 1 KHz respectively. G_{12} and C_{12} means value of conductance and capacitance between electrodes 1 and 2 respectively. Unit of conductance is nano- Siemens (nSie) and unit of capacitance is femto-farad (fF).

Table 3.4 and 3.6 shows the value of electrode's impedance for normal and cancer lung tissue cases at 1 MHz frequency calculated from table 3.3 and 3.5 data tables. Impedance was calculated using equations 3.1 and 3.3. It was assumed that the tissues have no or negligible inductive influence. Also, a column of relative difference of normal and cancer tissue cases for each electrode is also given. Graphical representation and explanation of following tables are given in section 5.1.

Table 3.3: Value of conductance and capacitance of the simulation design for normal and cancer lung cases respectively at 1 MHz frequency

Electrodes	Conductance G (nSie)	Capacitance C (fF)	Conductance G (nSie)	Capacitance C (fF)
	Normal Lung Tissue		Cancer Lung Tissue	
(G_{12}, C_{12})	18.56	11.56	26.5	13.03
(G_{13}, C_{13})	13.82	4.17	16.85	5.38
(G_{14}, C_{14})	10.43	1.91	11.74	1.98
(G_{15}, C_{15})	13.97	4.04	16.01	5.51
(G_{16}, C_{16})	18.42	11.63	26.1	13.47

Table 3.4: Impedance value of electrodes for normal and cancer case simulation, calculated from data table 3.3

Electrodes	Impedance for normal case (MΩ)	Impedance for cancer case (MΩ)	Relative difference of impedance ((%))
Z_{12}	55.61	39.67	28.7
Z_{13}	81.81	66.34	18.92
Z_{14}	127.03	117.1	7.84
Z_{15}	81.71	68.82	15.8
Z_{16}	55.99	40.1	28.4

Table 3.5: Value of conductance and capacitance of the simulation design for normal and cancer lung cases respectively at 1 KHz frequency

Electrodes	Conductance G (nSie)	Capacitance C (fF)	Conductance G (nSie)	Capacitance C (fF)
	Normal Lung Tissue		Cancer Lung Tissue	
(G_{12}, C_{12})	0.054	32.17	0.098	37.89
(G_{13}, C_{13})	0.046	28.74	0.065	31.67
(G_{14}, C_{14})	0.036	24.09	0.039	28.79
(G_{15}, C_{15})	0.049	28.01	0.062	30.98
(G_{16}, C_{16})	0.056	32.01	0.092	28.75

Table 3.6: Impedance value of electrodes for normal and cancer case simulation, calculated from data table 3.5

Electrodes	Impedance for normal case (GΩ)	Impedance for cancer case (GΩ)	Relative Increment ((%))
Z_{12}	18.49	10.21	44.8
Z_{13}	21.74	15.38	29.23
Z_{14}	27.8	25.64	7.8
Z_{15}	20.41	16.13	20.97
Z_{16}	17.9	10.87	39.13

Chapter 4

Experimental Work

4.1 Introduction

Marchal et al., (1989)[11] suggested the use of gelatin phantoms for replicating dielectric properties of human tissues. Those low cost and low maintenance phantoms were made of gelatin and water. Gelatin phantom adopt various shapes depending on the organ to be simulated. Based on this idea, gelatin phantoms were made and evaluated to get the dielectric properties. After that, samples that behaved like the normal and lung cancer dielectric properties from table 3.2, were used to evaluate the tool prototype impedance.

4.2 Experimental procedure

4.2.1 Initial testing

Using previous research of Marchal et al., (1989) [11] an experimental procedure to find the electrical properties of the gelatin mold was conducted. Gelatin phantoms were a mixture of pure gelatin, sodium chloride and water. The original test batch recipe is shown in table 4.1.

Table 4.1: Original recipe to create a phantom sample

	Gelatin (g)	Water (mL)	NaCl (g)
Test 1	5	25	0
Test 2	5	25	0.5
Test 3	5	25	1

The procedure used to create a sample and method of characterization for those samples are given below:

- Water was heated in a laboratory beaker past 150°F.
- Hot water was mixed with gelatin and NaCl. The amount of which, as mentioned above in table 4.1 were maintained carefully.
- The mixture was stirred and then kept into a freezer for at least 24 hours.
- A solid mixture was created and was ready for characterization for its dielectric properties.
- The samples were cut into a 3D rectangle shape where all dimensions were measured by electronic calipers.
- Conductive copper (Cu) tape was placed on both sides of the samples with wire connecting the Cu like fig. 4.1c
- These wires were connected to LCR meter (Agilent U1733 handheld LCR meter) (fig. 4.1a) to calculate capacitance and resistance of the sample.
- Dielectric constant or relative permittivity (K or ϵ_r) and electric conductivity (σ)of these samples were calculated using following equations:

$$K = C\frac{t}{A\epsilon_0} \tag{4.1}$$

$$\sigma = \frac{t}{RA} \tag{4.2}$$

where, A and t are the area and thickness of the test samples that were cut. Permittivity of free space, ϵ_0= 8.854*10-12 F/m, capacitance (C) and resistance (R) of these samples were obtained by LCR meter. This LCR meter was equipped with testing capacitance, resistance, phase, impedance, and inductance at 100 Hz, 120 Hz, 1 kHz, 10 kHz and 100 kHz frequencies respectively.

Figure 4.1: (a) $\frac{3}{8}$ inch PVC probe with four pairs of electrodes and connecting wires. Also, a Agilent U1733 handheld LCR meter (b) Gelatin phantom samples solidifying in the refrigerator (c) Initial gelatin sample, getting characterized

4.2.2 Final testing of Samples Characterization

Initial tests 1, 2 and 3 were conducted to calculate capacitance and resistance. Using equations 4.1 and 4.2, variation of conductivity and relative permittivity at 1 KHz were observed. After getting satisfactory variations, different compositions of samples (table 4.2), mainly varying amount of NaCl were done. All procedures that were explained in section 4.2.1, were followed. The value of electric conductivity and relative permittivity for each samples were calculated, recorded and then compared against normal and cancer lung tissue properties table 3.2.

Table 4.2: List of compositions of samples

Sample Number	Gelatin (g)	Water (ml)	NaCl (g)	Sample Number	Gelatin (g)	Water (ml)	NaCl (g)
Sample 1	5.07	25.5	0	Sample 5	5.01	25.2	1.5
Sample 2	5.03	25.3	0.51	Sample 6	5.03	25	2
Sample 3	5.01	25.4	1	Sample 7	5.01	24.9	2.5
Sample 4	5.03	25.1	1.25	Sample 8	5.04	25	2.75

Conductivity (σ) and relative permittivity (ϵ_r) of those eight samples and normal and cancer lung tissues are shown in fig. 4.2 and fig. 4.3. All samples reacted consistently with the different frequency used in the test (1 KHz, 10 KHz and 100 KHz). Phantom samples were able to get close to the relative permittivity and conductivity values provided by Wang et al. (2014) [2]. All values of σ and ϵ_r are grouped very closely in fig. 4.2 and fig. 4.3. The best mixture to represent the healthy lung tissue would be sample 5 which was composed of 5 grams of gelatin, 25 milliliters of water, and 1.25 grams of sodium chloride. Also, sample 8 represented cancer lung tissue very closely which was composed of 5 grams of gelatin, 25 milliliters of water, and 2.75 grams of sodium chloride. Value of conductivity of sample 8 was less than conductivity of cancerous lung tissue but, considering the variance in the measurement tools, this was the closest.

Impedance calculation of samples 5 and 8 using probe

Phantom samples 5 and 8 were chosen as normal and cancer lung tissue replica respectively. The next step was to calculate the impedance when the probe was inserted

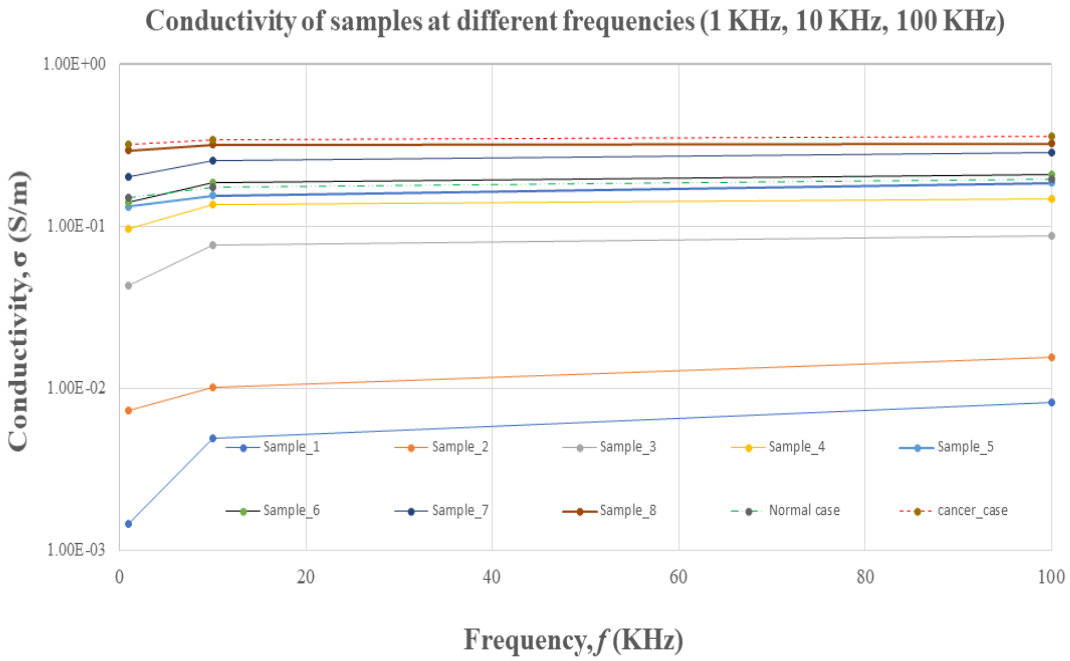

Figure 4.2: (a) Conductivity of samples at different frequencies (1 KHz, 10 KHz, 100 KHz)

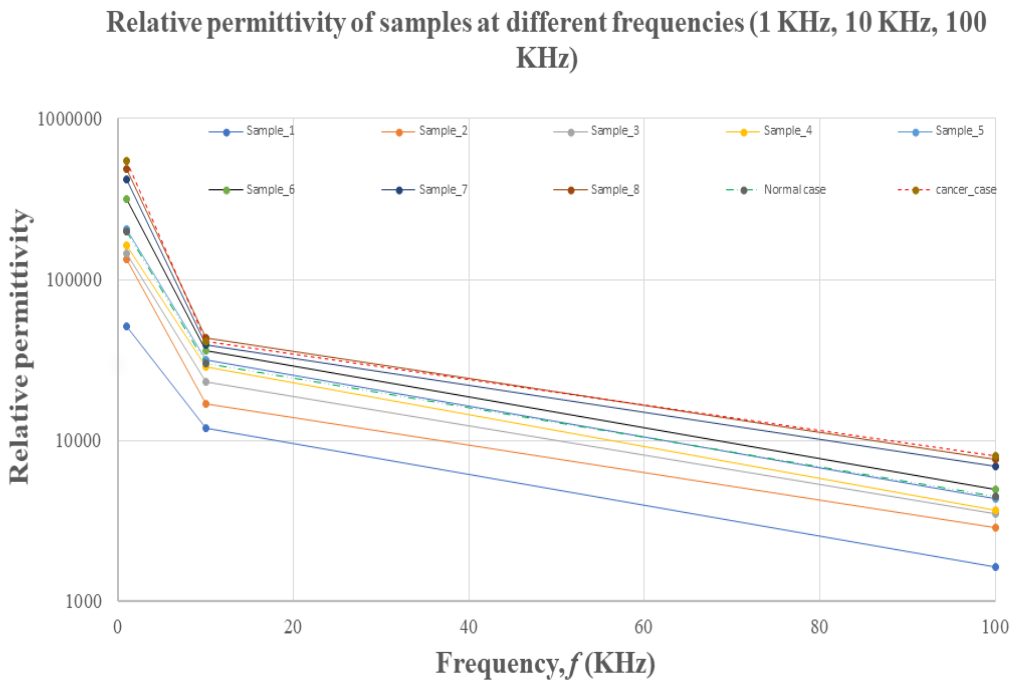

Figure 4.3: Relative permittivity of samples at different frequencies (1 KHz, 10 KHz, 100 KHz)

into those samples. The prototype probe was made of a polyvinyl chloride tubing with wires connecting to the top to create four pairs of copper electrodes (fig. 4.1a). The diameter of the probe was 0.375 inch. So, a 0.4 inch diameter aluminum bar was used to create smooth hole in the samples 5 and 8 so that the prototype probe can be inserted easily. Value of impedance (Z_{12}, Z_{13} and Z_{14}) at different electrodes position was recorded using LCR meter. Z_{12} is impedance at electrodes 1 and 2 position. Graphical representation and explanation of the final results were discussed in section 5.2.

Chapter 5

Results and Discussion

5.1 Simulation Results

- From fig 5.1, value of conductance from Ansys Q3D simulation, was higher for cancer cases than normal lung tissue case in each frequency. Also, the value of conductance for G_{12} was higher than G_{13} and G_{14}. That means, change of electrode position was a key factor in conductance values in addition to measurement frequencies.

- From fig 5.2, value of capacitance for cancer lung tissue case was higher than normal lung tissue case. Value of capacitance for C_{12} was higher than C_{13} and C_{14}. Value of capacitance was higher at high frequency also. From table 3.3, values of design capacitance of normal and cancer lung tissue simulation were really close at 1 MHz than 1 KHz. Capacitance of C_{16} at 1 KHz behaved inversely from the common trend of capacitance graph.

- From figure 5.3, it was evident that total impedance of simulation design for normal cases were higher than cancer cases. This information matched another result of the impedance of breast tissue under the scanning probe. Those impedance spectroscopy of breast tissue showed cancer (lower impedance) as bright, white spots on an otherwise gray background of normal or non-cancerous breast tissue (higher impedance) [37]. Value of impedance was also higher at low frequency

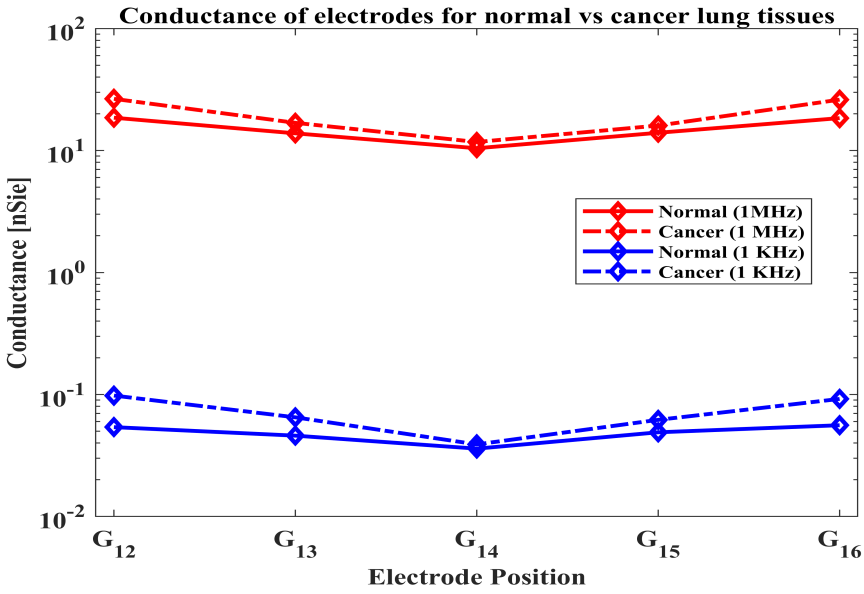

Figure 5.1: Value of conductance at different electrodes position for normal and cancer lung tissue case at 1 MHz and 1 KHz. G_{12} was the value of conductance at electrodes 1 and 2.

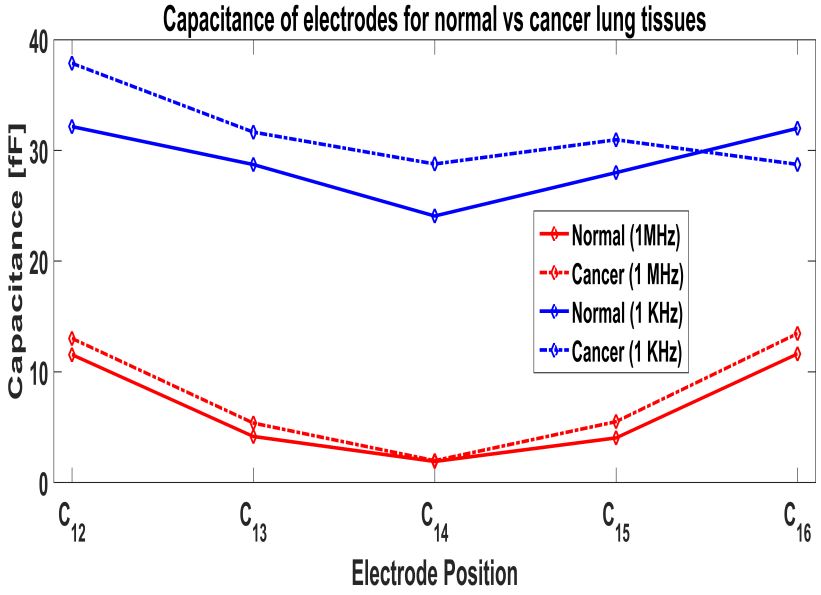

Figure 5.2: Value of capacitance at different electrodes position for normal and cancer lung tissue case at 1 MHz and 1 KHz. C_{12} was the value of capacitance at electrodes 1 and 2.

(f=1 KHz). Similarly, in this simulation, higher impedance was obtained for normal lung tissue case and lower impedance for cancer lung tissue case. Also, the value of impedance at electrodes 1 and 2, Z_{14} was higher than any other electrode positions.

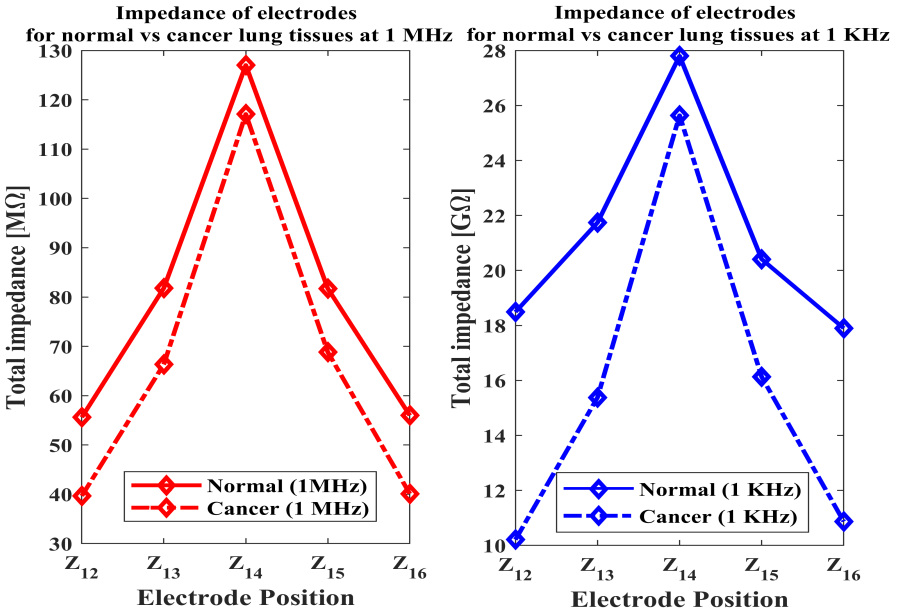

Figure 5.3: Value of impedance at different electrodes position for normal and cancer lung tissue case at 1 MHz and 1 KHz. Z_{12} was the value of impedance at electrodes 1 and 2.

5.2 Experimental Results

Gelatin phantom samples 5 and 8 were selected as normal and cancerous lung tissue, respectively, since these samples have the dielectric properties that are the closest match with normal and cancer lung tissue data. The final step of the experimental work was to find impedance value of the prototype probe for both samples using LCR meter. From figures 5.4, 5.5 and 5.6, main findings of this experiment were:

- Total impedance for sample 5 was always higher than sample 8.
- Impedance of Z_{13} was higher than other electrode positions.

- At low frequency like 1 KHz, impedance difference of different electrode positions were easily recognizable. But at higher frequency like 1 MHz, it was difficult to differentiate.
- Total impedance at higher frequency was in range of KΩ whereas it was MΩ at lower frequency.
- Theoretically value of Z_{12} and Z_{14} should be equal. But experimentally, it was never achieved. The impedance values were close but different.

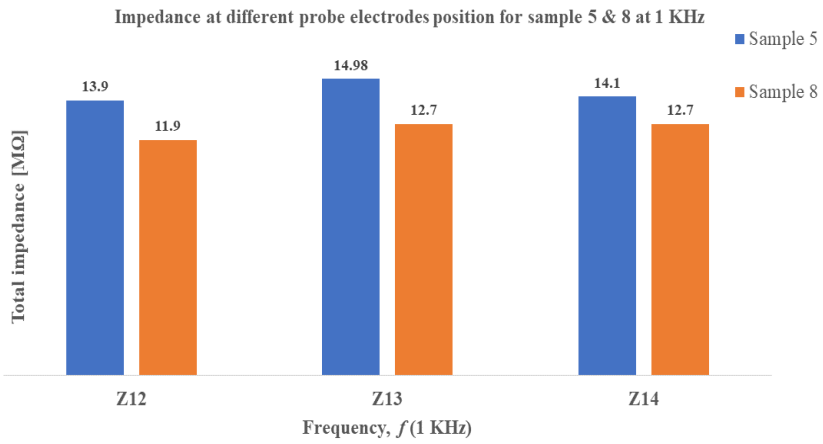

Figure 5.4: Impedance at different electrodes position (Z_{12}, Z_{13} and Z_{14}) for sample 5 and 8 at 1 KHz.

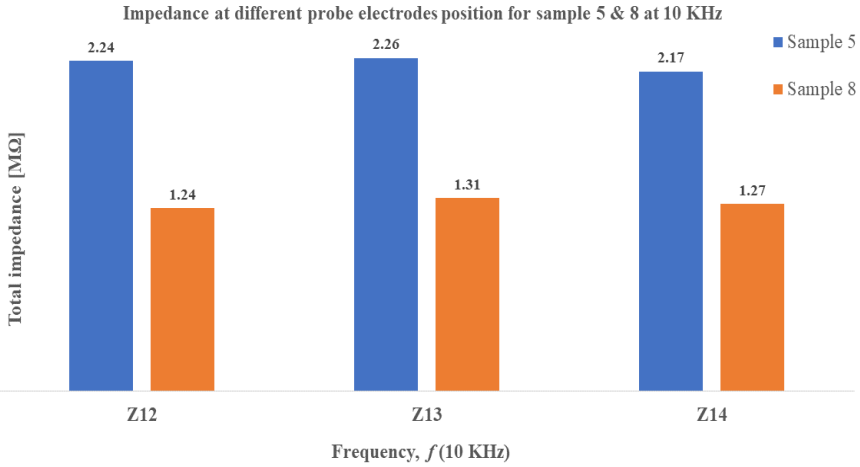

Figure 5.5: Impedance at different electrodes position (Z_{12}, Z_{13} and Z_{14}) for sample 5 and 8 at 10 KHz.

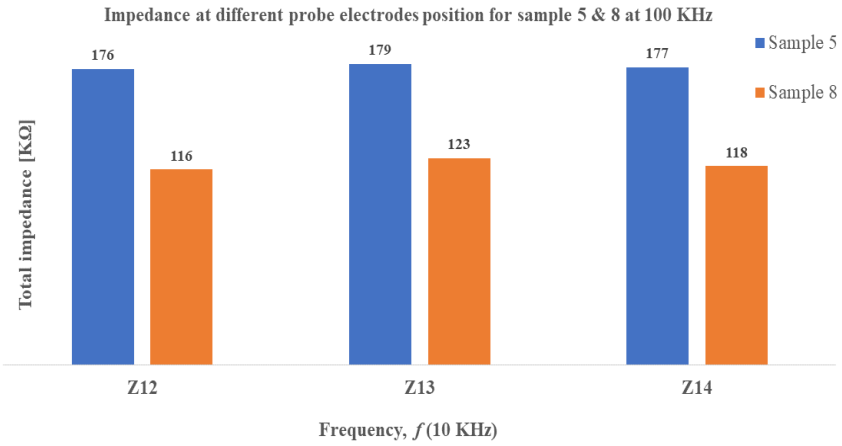

Figure 5.6: Impedance at different electrodes position (Z_{12}, Z_{13} and Z_{14}) for sample 5 and 8 at 100 KHz.

Table 5.1: Relative difference of sample 5 and 8 impedance values (%) at 1, 10 and 100 KHz frequencies

Frequency (KHz)	Relative difference of sample 5 and 8 impedance values (%)		
	Z_{12}	Z_{13}	Z_{14}
1	14.4	15.2	9.9
10	44.6	31.4	46.4
100	34.1	6.5	32.8

Chapter 6

Conclusion

This study demonstrated the possibility of using electrode impedance tomography for lung cancer biopsy. In the Q3D simulation, the relative difference in impedance between normal and lung cancer cases was obvious at different electrode positions and frequencies. At 1 MHz, the impedance difference between Z_{12} and Z_{14} was 71.42 MΩ for normal case and 77.43 MΩ for cancer case simulation. At same frequency, the relative difference between normal and cancer case of Z_{12} was 28.7%. At 1 KHz, the difference between Z_{12} and Z_{14} was 9.31 MΩ for normal case and 15.43 MΩ for cancer case simulation. At same frequency, the relative difference between normal and cancer case of Z_{12} was 44.8% which was higher than 1 MHz simulation case.

Experimental impedance of samples 5 and 8 were also different. Total impedance was higher at 1 KHz same as simulation results. But The relative difference between sample 5 and 8 impedance values were higher at 10 KHz and also 100 KHz than 1 KHz (table 5.1). So, evaluating value at higher frequency is more helpful to differentiate normal and cancerous lung tissue impedance.

In addition, the use of electrodes for impedance measurement in lung biopsy tools is a promising idea. Future ideas may improve this situation:

- All those simulations were performed for a filling factor (ratio of air volume to lung tissue volume) of 0.1781. Therefore, all simulation data used were from a specific lung case. Therefore, more simulations are needed on different filling factors to better understand impedance tomography.

- Gelatin phantom model was used because of it's availability and low cost. It was a very difficult task to select samples that behave like normal and cancer lung tissue properties. Different kinds of manufactured phantom samples might be useful to get more accurate data.

- The LCR meter that was used in this experiment, was showing fluctuating readings. Better filtering or time averaging to cancel all noise may be useful to get accurate results.

- In the future, simulation and experimental works can be carried out according to the tissue characteristics of different lung cancer stages. This idea would be helpful to gather more knowledge on impedance spectroscopy.

References

[1] Round wire ac resistance calculator. https://chemandy.com/calculators/round-wire-ac-resistance-calculator.htm. (Accessed on 08/06/2020).

[2] Jie-Ran Wang, Ben-Yuan Sun, Hua-Xiang Wang, Shan Pang, Xiao Xu, and Qing Sun. Experimental study of dielectric properties of human lung tissue in vitro. *Journal of Medical and Biological Engineering*, 34(6):598–604, 2014.

[3] Gills Fai, Sarah Ostlie, Michael Greminger, Roy Cho, and H Erhan Dincer. Tool for transbronchial biopsies of peripheral lung nodules. In *2019 Design of Medical Devices Conference*. American Society of Mechanical Engineers Digital Collection, 2019.

[4] Basics of measuring the dielectric properties of materials. https://www.cmc.ca/wp-content/uploads/2019/08/Basics_Of_MeasuringDielectrics_5989-2589EN.pdf. Accessed: 2019-07-29.

[5] Rebecca L Siegel, Kimberly D Miller, Stacey A Fedewa, Dennis J Ahnen, Reinier GS Meester, Afsaneh Barzi, and Ahmedin Jemal. Colorectal cancer statistics, 2017. *CA: a cancer journal for clinicians*, 67(3):177–193, 2017.

[6] Home — american cancer society - cancer facts & statistics. https://cancerstatisticscenter.cancer.org/#!/. (Accessed on 07/29/2020).

[7] How to detect non-small cell lung cancer — lung cancer tests. https://www.cancer.org/cancer/lung-cancer/detection-diagnosis-staging/how-diagnosed.html. (Accessed on 07/30/2020).

[8] Luis M Seijo. Electromagnetic navigation bronchoscopy: clinical utility in the diagnosis of lung cancer. *Lung Cancer: Targets and Therapy*, 7:111, 2016.

[9] Ralf Eberhardt, Devanand Anantham, Armin Ernst, David Feller-Kopman, and Felix Herth. Multimodality bronchoscopic diagnosis of peripheral lung lesions: a randomized controlled trial. *American journal of respiratory and critical care medicine*, 176(1):36–41, 2007.

[10] Tushar Kanti Bera. Bioelectrical impedance methods for noninvasive health monitoring: a review. *Journal of medical engineering*, 2014, 2014.

[11] Christian Marchal, Mustapha Nadi, AJ Tosser, Catherine Roussey, and Marie Louise Gaulard. Dielectric properties of gelatine phantoms used for simulations of biological tissues between 10 and 50 mhz. *International journal of hyperthermia*, 5(6):725–732, 1989.

[12] Carl H Durney, Habib Massoudi, and Magdy F Iskander. Radiofrequency radiation dosimetry handbook. Technical report, UTAH UNIV SALT LAKE CITY DEPT OF ELECTRICAL ENGINEERING, 1986.

[13] KR Foster and HP Schwan. Dielectric properties of tissues. handbook of biological effects of electromagnetic fields. *CRC Press, Boca Raton, New York, London, Tokio*, pages 25–102, 1996.

[14] Camelia Gabriel, Sami Gabriel, and y E Corthout. The dielectric properties of biological tissues: I. literature survey. *Physics in medicine & biology*, 41(11):2231, 1996.

[15] William T Joines, Yang Zhang, Chenxing Li, and Randy L Jirtle. The measured electrical properties of normal and malignant human tissues from 50 to 900 mhz. *Medical physics*, 21(4):547–550, 1994.

[16] Suguru Kimura, Tadaoki Morimoto, Tadashi Uyama, Yasumasa Monden, Yohsuke Kinouchi, and Tadamitsu Iritani. Application of electrical impedance analysis for diagnosis of a pulmonary mass. *Chest*, 105(6):1679–1682, 1994.

[17] Jianling Gao, Shihong Yue, Jun Chen, and Huaxiang Wang. Classification of normal and cancerous lung tissues by electrical impendence tomography. *Bio-medical materials and engineering*, 24(6):2229–2241, 2014.

[18] A Borsic, R Halter, Y Wan, A Hartov, and KD Paulsen. Electrical impedance tomography reconstruction for three-dimensional imaging of the prostate. *Physiological measurement*, 31(8):S1, 2010.

[19] Kenneth S Cole and Howard J Curtis. Electric impedance of single marine eggs. *The Journal of general physiology*, 21(5):591, 1938.

[20] Kenneth S Cole and Rita M Guttman. Electric impedance of the frog egg. *The Journal of general physiology*, 25(5):765–775, 1942.

[21] Wallace H Coulter. High speed automatic blood cell counter and cell size analyzer. In *Proceedings of the National Electronics Conference*, volume 12, page 1034, 1956.

[22] RA Hoffman and WB Britt. Flow-system measurement of cell impedance properties. *Journal of Histochemistry & Cytochemistry*, 27(1):234–240, 1979.

[23] Ivar Giaever and Charles R Keese. Monitoring fibroblast behavior in tissue culture with an applied electric field. *Proceedings of the National Academy of Sciences*, 81(12):3761–3764, 1984.

[24] K Ikuta and K Hirowatari. Real three dimensional microfabrication using stereolithography and metal molding proc. In *IEEE Conf. on Microelectromechanical Systems (Piscataway, NJ: IEEE) p*, volume 42, 1993.

[25] David C Duffy, J Cooper McDonald, Olivier JA Schueller, and George M Whitesides. Rapid prototyping of microfluidic systems in poly (dimethylsiloxane). *Analytical chemistry*, 70(23):4974–4984, 1998.

[26] J Cooper McDonald, David C Duffy, Janelle R Anderson, Daniel T Chiu, Hongkai Wu, Olivier JA Schueller, and George M Whitesides. Fabrication of microfluidic systems in poly (dimethylsiloxane). *ELECTROPHORESIS: An International Journal*, 21(1):27–40, 2000.

[27] Richard H Bayford. Bioimpedance tomography (electrical impedance tomography). *Annu. Rev. Biomed. Eng.*, 8:63–91, 2006.

[28] Khalil Heileman, Jamal Daoud, and Maryam Tabrizian. Dielectric spectroscopy as a viable biosensing tool for cell and tissue characterization and analysis. *Biosensors and Bioelectronics*, 49:348–359, 2013.

[29] B Lamprecht, P Porsch, B Wegleitner, G Strasser, B Kaiser, and M Studnicka. Electromagnetic navigation bronchoscopy (enb): Increasing diagnostic yield. *Respiratory medicine*, 106(5):710–715, 2012.

[30] David W Hsia, Kurt W Jensen, Douglas Curran-Everett, and Ali I Musani. Diagnosis of lung nodules with peripheral/radial endobronchial ultrasound-guided transbronchial biopsy. *Journal of bronchology & interventional pulmonology*, 19(1):5–11, 2012.

[31] Andy Adler and Alistair Boyle. Electrical impedance tomography: Tissue properties to image measures. *IEEE Transactions on Biomedical Engineering*, 64(11):2494–2504, 2017.

[32] RA Nicholson and M Crofton. Training phantom for ultrasound guided biopsy. *The British Journal of Radiology*, 70(830):192–194, 1997.

[33] Hirokazu Kato and Tetsuya Ishida. Development of an agar phantom adaptable for simulation of various tissues in the range 5-40 mhz.(hyperthermia treatment of cancer). *Physics in Medicine & Biology*, 32(2):221, 1987.

[34] J Ross Macdonald. Impedance spectroscopy. *Annals of biomedical engineering*, 20(3):289–305, 1992.

[35] Franco Simini and Pedro Bertemes-Filho. *Bioimpedance in biomedical applications and research*. Springer, 2018.

[36] Dielectric properties it'is foundation. `https://itis.swiss/virtual-population/tissue-properties/database/dielectric-properties/`. (Accessed on 08/10/2020).

[37] What is electrical impedance? — t scan — imaginis - the women's health & wellness resource network. https://imaginis.com/t-scan/what-is-electrical-impedance?fbclid=IwAR3gw5kxqAV5yQE6eCbArBm2YGOuKbn7K4bY77vw8IyMHCPH3LpwnbsUaNo. (Accessed on 08/09/2020).